CHAPTER 3

AFM Force Measurement for Activated Sphalerite-Xanthate Interactions

3.1 INTRODUCTION

Unlike most other sulfide minerals, sphalerite responds poorly to short-chain thiol collectors. The problem is attributed to the high solubility of zinc-thiol compounds in water [1]. Also, due to its large band gap (3.7 eV), sphalerite is a poor catalyst for mixed potential reactions between xanthate and oxygen [2].

The reactivity of sphalerite with xanthate improves when the mineral is activated by heavy metal ions, such as copper, to form a copper sulfide, as follows:

$$ZnS_{(s)} + Cu^{2+}_{(aq)} \rightarrow CuS_{(s)} + Zn^{2+}_{(aq)} \qquad [1]$$

which in turn reacts with the collector to form stable copper xanthate to render the mineral surface hydrophobic.

It is well known that sphalerite flotation is sensitive to pH. Kartio, et al. [3] conducted XPS studies on copper-activated sphalerite in alkaline pH. The results showed that a CuS-like activation product is formed in deoxygenated solutions, while copper polysulfide is formed in air-saturated solutions. This finding provides an explanation for the collectorless flotation of copper-activated sphalerite [4-6]. Other investigators [7,8] identified elemental sulfur, rather than the polysulfide, as the hydrophobic species when sphalerite was copper-activated in acidic solutions. More information about the various activation products of sphalerite can be obtained from a recent review by Finkelstein [9] where this topic has been dealt with comprehensively.

It is well known that sphalerite flotation is difficult in the neutral pH range. Sutherland and Wark [10,11] attributed the difficulty to the precipitation of copper xanthate, which in turn depletes the solution of xanthate ions. The Hallimond tube flotation experiments conducted by Steininger [12] showed that sphalerite flotation is suppressed in the pH range of 6 to 9. The higher the copper sulfate addition, the wider the pH range of flotation suppression became. Steininger attributed the suppression to the formation of a basic copper xanthate ($Cu_2(OH)_2X_2$), rather than the copper xanthate, at the near neutral pH. Laskowski and co-workers [13,14] also showed the difficulty in floating sphalerite at near neutral pH, and attributed it to the presence of $CuOH^+$ ions which, according to the authors, do not form a 'flotation active' activation product such as CuS on the surface of sphalerite. These authors showed, however, that the sphalerite flotation at neutral pH improves after a long conditioning time.

It is the objective of the present work to study the mechanism of sphalerite flotation by measuring the surface forces relevant to bubble-particle interactions. Many investigators conducted direct force measurements between two solid surfaces using surface force apparatus (SFA) [15-22] and atomic force microscope (AFM) [23-28]. Some investigators [29-32] extended these techniques to directly measure the surface forces between air bubbles and solid surfaces. However, the measurement proved to be more difficult than anticipated. In a given force measurement, a bubble surface deforms as it approaches a solid surface, which makes it difficult to accurately determine the distance separating the air bubble and solid surface. Consequently, there are considerable discrepancies among the results reported by different investigators. Furthermore, some of the results are not consistent with previous work reported in flotation literature. To alleviate the problem associated with the deformation of bubble surface, force measurements were conducted [33,34] using a hydrophobized glass sphere as a 'simulated' air bubble. This technique is based on the finding that an air bubble is inherently hydrophobic [35-39]. Furthermore, recent spectroscopic studies by Quan et al [40] suggest that the orientation of water molecules adjacent to a silanated hydrophobic solid surface is identical to that at the air/water interface.

Using the technique suggested above, the force measurements conducted for the quartz/amine [33] and covellite/xanthate [34] systems were found to be consistent with the respective flotation data.

In fact this technique is gaining acceptance in the scientific community as is evidenced by the recent work of Nalkowski et al [41] who conducted force measurements between a colemanite surface and a hydrophobic polyethylene sphere in aqueous solution. These investigators found the results of force measurements to be consistent with colemanite flotation data.

Surface forces (F) measured using either SFA or AFM are routinely analyzed using the DLVO theory [42,43]:

$$F = F_e + F_d \qquad [2]$$

in which F_d is the London-van der Waals dispersion force and F_e is the ion-electrostatic force. The magnitude of the former is represented by the Hamaker constant (A), while that of the latter is represented by the double-layer potential (ψ). However, according to Derajaguin and Churaev [44] the DLVO theory is applicable only to those colloidal particles whose water contact angles (θ) are in the range of 20-45°. Therefore, for strongly hydrophobic surfaces, it is necessary to extend the theory by including the contributions from the hydrophobic forces (F_h), as follows:

$$F = F_e + F_d + F_h \qquad [3]$$

which is frequently referred to as extended DLVO theory. It has been shown that the hydrophobic forces can be conveniently represented in the form of a power law [25, 26,45] such as:

$$F_h = -\frac{R.K}{6H^2} \qquad [4]$$

in which R is the radius of curvature of the spherical (or cylindrical) object used for direct force measurement, H is the closest distance separating the two surfaces, and K is a constant. Eq. [4] is of the same form as the one commonly used for the dispersion force. Therefore, K can be directly compared with A.

In the present work, direct force measurements were conducted between hydrophobized glass sphere and sphalerite plate using an AFM. The measurements were conducted to study the effects of pH on the magnitudes of the hydrophobic forces observed in the presence of potassium ethyl xanthate. Other investigators [46-49] also measured surface forces using zinc sulfide spheres; however, none of these measurements were conducted in the presence of xanthates.

3.2 EXPERIMENTAL

3.2 (a) Materials

Specimen-grade sphalerite from Santander, Spain, was obtained from the Ward's Natural Science Est. The sphalerite surface was wet-polished, first, using 600 grit silicon carbide paper and, then, using 3-micron Buehler silicon carbide paper. The final polishing was done on Buehler polishing cloth using an aluminum oxide (30 nm) suspension. After polishing, the sample was cleaned in an ultrasonic bath for 5 minutes. The polished mineral surface was then rinsed with ethanol and then dried by blowing nitrogen. The method employed for polishing the mineral surface is very similar to that used by Drelich, et al [50]. These investigators found that such a method of polishing produces surface with very low surface roughnesses (R_{max}<10 nm). The polished sphalerite surface was used as a plate in AFM force measurements. The AFM image of the sphalerite samples prepared in a manner described above showed a maximum peak to valley roughnesses in the range of 10 nm over a scan area of 400×400 nm^2. Thus, the surfaces would not be smooth enough to measure the forces in short separation distances; however, the forces measured at longer separation distances may be reliable.

Glass spheres were obtained from Duke Scientific. They were hydrophobized by octadecyltrichlorosilane (OTS), and used for the force measurements. The OTS was obtained from Aldrich Chemical Company at 95% purity and used without further purification. The glass spheres, as received, were reacted with OTS in HPLC grade cyclohexane, which was obtained from Aldrich Chemical Company. Flinn, et al. [51] described the method of hydrophobizing glass spheres in detail.

For each experiment, a hydrophobized glass sphere was glued to the end of an AFM cantilever spring by means of Epon R Resin 1004F from Shell Chemicals Company. The cantilever springs used in the force measurements included Tapping Etched Silicon Probes (TESP), Force Etched Silicon Probes (FESP) and regular silicon nitride tips, which were obtained from Digital Instruments, Santa Barbara, CA.

Force measurements were conducted in solutions of potassium ethyl xanthate (KEX). All of the solutions were prepared using the conductivity water from a Barnstead Nanopure II water purification system. The pH of the KEX solutions were adjusted by adding aliquots of reagent-grade NaOH and/or HCl solutions. The KEX used in the present work was obtained by dissolving an industrial-grade reagent in acetone and recrystallyzing it in ether.

3.2 b Apparatus and Procedure

Figure 3.1 shows a schematic representation of the atomic force microscope (AFM), Digital Instruments Nanoscope III scanning probe microscope, that was used for direct force measurements. A hydrophobic glass sphere (a), which represents an air bubble in flotation, is attached at the end of a cantilever spring (b). A polished sphalerite plate (c) is placed on a piezo-electric crystal (d), which is designed to move the mineral relative to the glass sphere. If a repulsive force exists between the glass sphere and the sphalerite plate, the cantilever will be deflected upward. On the contrary, if there exists an attractive force between the sphere and plate, the cantilever will be deflected downward. The cantilever deflection is monitored by the laser beam, which is emitted by its source (e), deflected off the cantilever, and enters a detector (f). From the cantilever deflection, one can determine i) the closest distance (H) between the glass sphere and sphalerite plate, and ii) the force (F) between the two surfaces if the spring constant of the cantilever is known. In the present work, the spring constants were determined using the technique described by Senden and Ducker [52]. For the measurement of repulsive forces, the standard triangular silicon nitride (Si_3N_4) cantilevers ($0.1 \leq k \leq 0.32$ mN/m) were used. To measure strong attractive forces, rectangular TESP ($25 \leq k \leq 35$ mN/m) and FESP ($5 \leq k \leq 7$

mN/m) cantilevers were used. All experiments were conducted in aqueous media using a liquid cell provided by Digital Instrument. Further details of the experimental technique can be obtained from references [25] and [34].

3.2 c Contact Angle Measurements

Equilibrium contact angles of a polished sphalerite electrode were measured using the captive bubble technique by means of a Rame-Hart Model 100 goniometer. The electrode was immersed in a solution of interest, with its polished surface facing down and an air bubble approaching the surface from below. The angles were measured through the aqueous phase.

The contact angle of the hydrophobized glass sphere was determined by conducting the measurement on a glass plate that had been hydrophobized in the same OTS solution as that used for the glass sphere. The sessile drop technique was used for the measurement. The glass spheres, whose contact angle (q) is 109^{o}, were used as simulated air bubbles in the surface force measurements.

The Hamaker constant of the sphalerite sample was calculated from its methylene iodide contact angle, as described previously [53,54, 34]. The contact angle was determined using the sessile drop technique.

3.2 d Measurements of the Electrochemical Potentials of Sphalerite

The electrochemical potentials of sphalerite electrodes were measured using a carbon-matrix composite (CMC) electrode [55]. This electrode was prepared by mixing sphalerite particles (105-150 μm) with a graphite powder along with a conducting resin. The use of CMC:ZnS electrode allowed the measurements of the electrochemical potentials of activated sphalerite particles.

3.3 RESULTS AND DISCUSSION

3.3 a Force measurements conducted at pH 9.2

Figure 3.2 shows the results of the direct surface force measurements conducted between a polished sphalerite plate and a hydrophobized glass sphere in a 10^{-3} M KEX solution. As has already been noted, the hydrophobic glass sphere may represent a simulated air bubble. Thus, the results of the force measurement may reveal information pertaining to the bubble-particle interactions occurring during flotation. The measured forces (F) were normalized by the radius (R) of the sphere, and are plotted versus the closest separation distance (H) between the sphalerite plate and the simulated air bubble. Two sets of force data are given in Figure 3.2. One was obtained with unactivated sphalerite, and the other was obtained with copper-activated sphalerite. The force data obtained with the unactivated sphalerite (upper curve) can be fitted to the DLVO theory (solid line) (Eq. [2]). The data have been fitted to the constant charge model [56] using the following parameters: surface potential of sphalerite $\psi_{1(\infty)} = -63$ mV; surface potential of glass sphere $\psi_{2(\infty)} = -60$ mV, κ^{-1} (Debye length) = 9.1 nm and A_{132} (Hamaker constant) = 0.8×10^{-20} J.

It needs to be stressed that the force data presented in Figure 3.2 are for the interaction between two dissimilar surfaces, i.e., two surfaces interacting with unequal but constant charge densities. This means that the data cannot be fitted to the theory assuming that there exists only one set of unique double layer potential values [57-60]. Therefore, to avoid any ambiguity, the surface potential of at least one of the surface should be known *a priori* before the data can be meaningfully fitted to the DLVO theory [57-60]. In the present case the surface potential of the OTS-coated glass surface was determined as follows: Force measurements were conducted between hydrophilic silica/silica surfaces for a given pH in 10^{-3} M KEX solution. The force data were fitted to the DLVO theory to obtain the values of the surface potential. The surface potential values for the OTS-coated glass sphere were assumed to be the same as that obtained from force measurements of hydrophilic silica, for a given experimental condition. This is a well-justified assumption since silanation is not known to change the surface potential of silica [61]. Note that the OTS coated surfaces were not directly used since the

interaction results in strong net hydrophobic forces that cannot be fitted to the DLVO theory [26]. In the rest of this communication, for a given experimental condition, the procedure outlined above has been adopted to determine the surface potential of the OTS-coated glass sphere.

It needs to be pointed out that the London van der Waals force (F_d) was calculated using A_{132} (Hamaker constant) = 0.8×10^{-20} J. Here, the value of A_{132} represents the van der Waals interaction between the sphalerite plate **1** and the glass sphere **2** in an aqueous medium **3**. Its value was determined using the combining law:

$$A_{132} = \sqrt{A_{131}.A_{232}} \qquad [5]$$

where A_{131} is the Hamaker constant for the interaction between two sphalerite surfaces in an aqueous medium and A_{232} is the same between two glass spheres. The value of A_{131} was obtained from the methylene iodide contact angle (20^o) determined in the present work, while the value of A_{232}($=0.8\times10^{-20}$ J) was taken from the literature [62].

An interesting observation from Figure 3.2 is that although the force data are well described by the DLVO theory at large separations, there exists an extraneous repulsive force at short separation distance (H<3 nm) which cannot be accounted for by the DLVO theory. It is believed that the surface roughness associated with the interacting surfaces effectively reduces the dispersion forces well below the sensitivity of the AFM, so that no jump into primary contact is observed [47-49]. However this behavior, as it will be evident in the ensuing sections, has very little consequence as far as the interpretation of the results in this work are considered.

Thus the force data obtained for the asymmetric interaction between the hydrophobic glass sphere and unactivated ZnS in xanthate solutions can be fitted to the DLVO theory (for H>3 nm). This is not surprising since the unactivated sphalerite plate exhibited contact angle of only 16^o (Table 3.1) in 10^{-3} M KEX solutions, i.e., the surface remains essentially hydrophilic. The absence of a hydrophobic force is consistent with observations reported in literature [34, 63,64] where the interaction between a

hydrophobic and a hydrophilic surface is shown to be adequately described by the DLVO theory. However, this is contradictory to the observations made by Tsao et al [23, 65] who suggest that strong hydrophobic forces can exist for the interaction between a hydrophobic and hydrophilic surface. Although the issue is far from resolved, it needs to be pointed out that the data presented here is definitely more relevant from a flotation perspective, since good flotation recoveries cannot be achieved using a mineral surface that is essentially hydrophilic.

The lower force curve in Figure 3.2 shows the force data obtained with copper-activated sphalerite in a 10^{-3} M KEX solution. The sphalerite plate had been activated in a 10^{-4} M $CuSO_4$ solution at pH 9.2 for 15 minutes prior to the force measurement. The measured forces are net-attractive and could not be fitted to the DLVO theory. The force data have been fitted to the extended DLVO theory (Eq. [3]), which incorporates a hydrophobic force term. In the present work, a power law (Eq. [4]) was used to fit the measured hydrophobic force, with $K_{132}=3.0\times10^{-18}$ J (F_e and F_d values used are the same as that for the upper force curve in Figure 3.2). This value is 375-times larger than the Hamaker constant (A_{132}). The appearance of the hydrophobic force can be attributed to the adsorption of xanthate on the activated sphalerite. The contact angle of the activated sphalerite in the 10^{-3} M KEX solution was 65^o, which is much larger than that of the unactivated sphalerite.

It has been shown that sphalerite is activated via. reaction [1] at pH 9.2 [66]. The activation product (CuS) reacts with xanthate ion (X^-) to form insoluble copper-xanthate via. the following electrochemical reaction:

$$CuS + X^- \rightarrow CuX + S^0 + e \qquad [6]$$

According to the thermodynamic data given by Young [67], the reversible potential for this reaction is 0.147 V (SHE) at 10^{-3} M KEX. This potential is close to the rest potential (163 mV, SHE) measured by means of a CMC:ZnS electrode that had been activated in a 10^{-4} M $CuSO_4$ solution at pH 9.2 and then immersed in a 10^{-3} M KEX solution at the same pH.

It needs to be mentioned that some investigators [68-70] have also suggested the formation of dixanthogen as a possible hydrophobic species on activated sphalerite. Therefore dixanthogen formation according to the following electrochemical reaction:

$$X^- \rightarrow X_2 + 2e \qquad [7]$$

was also considered. However, the thermodynamically calculated value for the reversible potential for reaction [7] is 0.266 V (SHE) at 10^{-3} M KEX [34, 67] which is much higher than the rest potential of 163 mV (SHE) measured using a CMC:ZnS electrode. This suggests that the formation of dixanthogen according to reaction [7] is thermodynamically unfavorable. We therefore conclude that CuX must be the hydrophobic species formed on activated sphalerite at pH 9.2.

The value of K_{132}=3.0×10^{-18} J determined from the direct force measurement was for the asymmetric hydrophobic interaction between xanthate-coated sphalerite and OTS-coated glass sphere. This value may be used to calculate the hydrophobic force constant, K_{131}, for the symmetric interactions between two xanthate-coated sphalerite plates in water. This can be done using the combining law for hydrophobic force constants [26,71]:

$$K_{132} = \sqrt{K_{131}.K_{232}} \qquad [8]$$

where K_{232} is the hydrophobic force constant for the interaction between two silica plates. Although there is no theoretical basis for Eq. [8], its validity has been demonstrated in experiment. Substituting the values of K_{232} (=2×10^{-16} J) and K_{132} (=3.0×10^{-18} J) into Eq. [8], one obtains the value of K_{131} to be 4.5×10^{-20} J. The value of K_{232} used in this calculation is the same as that used by Yoon and Pazhianur [34]. The calculated value of K_{131} is approximately 5.6 times greater than A_{131}(=0.8×10^{-20} J).

3.3 (b) Force measurements conducted at pH 6.8

Figure 3.3 shows the *F/R* vs *H* curves obtained for the interaction between a polished unactivated sphalerite plate and a hydrophobized glass sphere in a 10^{-3} M KEX solution at pH 6.8. The

lower curve in Figure 3.3 represents the force data obtained using unactivated sphalerite. The data obtained at large separation distances can be fitted to the DLVO theory (constant charge model) with the following parameters: $\psi_{1(\infty)}$=−34 mV, $\psi_{2(\infty)}$=−54 mV, κ^{-1}=9.8 nm, and $A_{132}=0.8\times10^{-20}$ J. However, the data obtained at short separation distances (H<3 nm) deviate considerably due to the surface roughness of the sphalerite plate. The upper curve in Figure 3.3 shows the results obtained with activated sphalerite in a 10^{-3} M KEX solution. The sphalerite plate was activated in a 10^{-4} M $CuSO_4$ solution at pH 6.8 for 15 minutes. At large separation distances, the force data can be fitted to the DLVO theory with the following parameters: $\psi_{1(\infty)}$= −51 mV, $\psi_{2(\infty)}$= −54 mV, κ^{-1}=10.1 nm, and $A_{132}=0.8\times10^{-20}$ J. Again, the experimental data obtained at short separation distances deviate from the theory due to the surface roughness.

It is interesting to note that in the presence of 10^{-3} M KEX, $\psi_{1(\infty)}$ for activated sphalerite was considerably more negative (−51 mV) than that for unactivated sphalerite (−34 mV). It is likely that this increase in $-\psi_1$ is due to the adsorption of xanthate ions (X^-) on activated sphalerite. Similarly, the AFM force measurements conducted with covellite showed that $-\psi_1$ of covellite increased in the presence of xanthate [32]. It is not surprising that sulfide minerals, which are usually negatively charged at neutral pH, become more negative upon adsorption of xanthate ions. Many investigators [72-74] showed actually that ζ-potentials of sulfide minerals become more negative upon xanthate adsorption.

Perhaps the most important observation that can be made from the data shown in Figure 3.3 is that there are no signs of hydrophobic forces, regardless of whether sphalerite is activated or not. Also, the contact angles were 15^o and 20^o with and without activation, respectively (Table 3.1). These findings are consistent with the experiences in flotation practice. As has already been discussed in this communication, it is difficult to float sphalerite in the near neutral pH range [10-12].

Voltammetry experiments conducted by Chen [75] showed that xanthate actually adsorbs on activated sphalerite at pH 6.8. Yet, the surface remains hydrophilic, as shown by the AFM force measurements conducted in the present work. These results suggest either:

1. that xanthate adsorbs as a hydrophilic complex, such as Cu(OH)X and/or $Cu_2(OH)_2X_2$, or

2. that hydroxy complexes such as $CuOH^+$ or $Cu_2(OH)_2^+$ ions co-adsorb with xanthate on the surface.

In the latter case, xanthate probably adsorbs as copper xanthate, which is hydrophobic; however, the presence of the hydroxy species renders sphalerite surface hydrophilic. At this point, it is not certain which of the two possibilities above would actually be the case. Both are different from the theory of Sutherland and Wark [10,11] that copper xanthate precipitates in solution, causing a depletion of xanthate ions. On the other hand, the second possibility suggested above is similar to the suggestion of Laskowski, et al. [13] that "flotation inactive" activation products are formed at the neutral pH.

3.3 (c) Force measurements conducted at pH 4.6

Figure 3.4 shows the results of the AFM force measurements conducted between a sphalerite plate and a hydrophobized glass sphere at pH 4.6. The upper most curve was obtained with activated sphalerite in 10^{-3} M KEX. The activation condition was the same as employed at the higher pHs. The measurements were conducted without potential control. The force data obtained at longer separation distances can be fitted to the DLVO theory using the following parameters: $\psi_{1(\infty)}$=−25 mV; $\psi_{2(\infty)}$=−40 mV, κ^{-1}=13.4 nm, and $A_{132}=0.8\times10^{-20}$ J. The deviation observed at shorter distances (H<3 nm) is due to the surface roughness, which is the same as at the higher pHs. The fact that the force data can be fitted to the DLVO theory at larger separation distances suggests that there are no evidence for hydrophobic force. Two possible reasons may be given. *One*, the electrochemical potential of the sphalerite may be too low for xanthate to adsorb on the activated sphalerite. *Two*, xanthate may have been decomposed in the acidic solution. It has been shown that the rate of xanthate decomposition increases sharply with decreasing pH [76,77]. The potential measured with the CMC:ZnS electrode was 155 mV, which is slightly higher than the reversible potential (147 mV, SHE) of reaction [6] at 10^{-3} M KEX. However, the reversible potential may actually be higher, if one considers that xanthate ions decompose rapidly at pH 4.6. Assuming that the residual xanthate concentration is 10^{-4} M, the reversible potential becomes 196 mV SHE. It is likely, therefore, that both of the reasons given above, namely, the low potential and the rapid xanthate decomposition, account for the absence of hydrophobic force.

The next set of force measurements was conducted by adding hydrogen peroxide (H_2O_2) in the presence of KEX so that the potential was raised to 480 mV SHE, as measured with the CMC electrode. The results of the force measurements are represented by the lowest curve in Figure 3.4. It shows net-attractive forces, indicating the presence of long-range attractive forces not accounted for by the DLVO theory. The force curve can be fitted to the extended DLVO theory by incorporating a hydrophobic force term (Eq. [3]) with $K_{132}=1.2\times10^{-18}$ J. This value is 150 times larger than the Hamaker constant (A_{132}). The appearance of the strong hydrophobic forces is consistent with the increase in contact angle of sphalerite (from 15 to 49^o) when the potential was raised. Note that for this particular condition the formation of both CuX (reaction 6) and dixanthogen (reaction 7) is thermodynamically favorable.

Many investigators showed that copper-activated sphalerite becomes hydrophobic even without the addition of collector [4, 7, 78-80]. Possible explanations include oxidation of the activation product to copper polysulfides or elemental sulfur. In order to study this possibility further, force measurements were conducted at a higher electrochemical potential. The potential was raised to 480 mV by adding H_2O_2 to a 10^{-4} M $CuSO_4$ solution at pH 4.6 in the absence of xanthate. The middle force curve of Figure 3.4 represents the results of the force measurements. As shown, strong net-attractive forces were observed. The force curve has been fitted to the extended DLVO theory by incorporating a hydrophobic force term (Eq. [3]) with $K_{132}=7.0\times10^{-19}$ J. This value is 87.5 times larger than the Hamaker constant (A_{132}). The appearance of the hydrophobic force is consistent with the increase in contact angle from 15 to 41^o when the potential was raised. The increase in contact angle and the appearance of the hydrophobic force may be attributed to the superficial oxidation of the activated sphalerite, which results in the formation of hydrophobic oxidation products such as elemental sulfur or metal polysulfides. At pH 4.6, elemental sulfur is the more likely hydrophobic species. In fact, Ralston, et al [7] used the technique of mass spectrometry to detect elemental sulfur on the surface of activated sphalerite in acidic solutions.

Thus, hydrophobic forces were observed for the asymmetric interactions between hydrophobic glass sphere (simulating air bubble) and activated sphalerite plate both in the presence and absence of xanthate. Note here that the hydrophobic force constant (K_{132}=1.2×10^{-18} J) obtained in the presence of xanthate is 1.7-times stronger than that (K_{132}=7.0×10^{-19} J) obtained in the absence. This difference may be attributed to the likelihood that copper xanthate (CuX) and dixanthogen render the activated sphalerite more hydrophobic than the elemental sulfur formed as a result of oxidation.

The values of K_{132} obtained at pH 4.6 were used to calculate the values of K_{131} using the combining rule (Eq. [7]) and are listed in Table 3.1. The value of K_{131} obtained in the presence and absence of KEX are 0.72×10^{-20} J and 0.25×10^{-20} J respectively, which are actually smaller than the Hamaker constant (A_{131} =0.8×10^{-20} J). One might think that these K_{131} values are small enough to be included as part of the uncertainties involved in determining A_{131}. However, there may be a significant difference between a zero value of K_{131} and a small but non-zero value of K_{131}. A zero value of K_{131} may suggest that the surface is truly hydrophilic and that water will have a high work of adhesion (W_a) on the surface. It is customary that W_a is subdivided into dispersion (W_a^d) and non-dispersion (W_a^{nd}) components, i.e.,

$$W_a = W_a^d + W_a^{nd} \qquad [9]$$

Laskowski [81] showed that a hydrophilic surface should have its non-dispersion component (W_a^{nd}) greater than zero, i.e.,

$$W_a^{nd} > 0 \qquad [10]$$

Therefore, it is important to point out that the small but non-zero value of K_{131} signifies that the surface has become hydrophobic, i.e.,

$$W_a^{nd} \to 0 \qquad [11]$$

It is evident from Eq. [8] that a zero value of K_{131} will give a zero value of K_{132} irrespective of the magnitude of K_{232}. This is exactly what has been observed in the present study. When a hydrophobic glass sphere (whose contact angle is 109^o) is brought to the vicinity of an unactivated ZnS plate, there was no hydrophobic interaction. On the other hand, even a small value of K_{131} results in a substantially large K_{132} value due to the extremely large value of K_{232} (=2×10^{-16} J). Thus, it is necessary that $K_{132}>0$ for hydrophobic interactions to occur. This is a simple fact mineral engineers have known for a long time, but is an important matter to discuss to better understand the nature of hydrophobic interactions in general.

Table 3.1 shows also that the value of K_{131} obtained at pH 9.2 is larger than those obtained at pH 4.6. This may be surprising in that the presence of hydroxide(s) at the higher pH should decrease the hydrophobicity of the xanthate-coated sphalerite surface. Two possible explanations may be given. *First*, xanthate adsorption at pH 9.2 may entail displacement of hydroxyl groups. *Second*, at pH 4.6 considerable amount of xanthate ions may have been decomposed, resulting in a low surface coverage.

3.4 SUMMARY AND CONCLUSIONS

An atomic force microscope (AFM) was used to measure the surface forces between a polished sphalerite plate and a hydrophobic glass sphere (θ=109^o). The latter may simulate the behavior of air bubbles in flotation. The forces measured between copper-activated sphalerite and the hydrophobic glass sphere in 10^{-3} M KEX solution at pH 9.2 cannot be fitted to the DLVO theory due to presence of hydrophobic force. A power law, which is of the same form as the one used for the van der Waals force, was used to represent the hydrophobic force. Its force parameter (K_{132}=3.0×10^{-18} J) is 375-times larger than the Hamaker constant (A_{132}),

At pH 6.8, the force curves obtained with copper-activated sphalerite in 10^{-3} M KEX solutions can be fitted to the DLVO theory. There are no evidences for hydrophobic force, which provides an explanation for the difficulty in floating sphalerite at neutral pH.

At pH 4.6, the force curves obtained with copper-activated sphalerite in 10^{-3} M KEX solutions showed the presence of hydrophobic forces that can be fitted with $K_{132}=1.2\times10^{-18}$ J. This value is considerably smaller than at pH 9.2, which may be attributed to the low surface coverage of copper xanthate on the sphalerite surface. The low coverage may be caused by the decomposition of xanthate at pH. 4.6. Long-range hydrophobic forces were also observed with copper-activated sphalerite at pH 4.6 in the absence of xanthate. However, the measured force ($K_{132}=7.0\times10^{-19}$ J) is weaker than in the presence of KEX. The hydrophobic forces observed in the absence of collector may be due to the elemental sulfur formed as a result of oxidation at the acidic pH.

The asymmetric force constants (K_{132}) obtained from the direct force measurements have been used to calculate the symmetric hydrophobic force constants (K_{131}) using the geometric mean combining rule. These values are in the range of $0.25\text{-}4.5\times10^{-20}$ J depending on the pH.

3.5 REFERENCES

1. Kakovskii, I. A., *Proceedings of the Second Int. Congress Surf. Acivity*, Butterworths, London, **4**, , 225-241 (1957).
2. Maust, E.E. and Richardson, P.E, *U.S. Bureau of Mines Report of Investigation 8108*, 1976.
3. Kartio, I. J., Basilio, C. I. and Yoon, R.H., In: *Proc. Int. Symp. Electrochemistry in Mineral and Metal Processing IV*, Richardson, P.E., Srinivasan, S. And Woods, R. Eds., Electrochem. Soc., Pennington, N.J., 25-37. (1996).
4. Yoon, R.-H., *International Journal of Mineral Processing*, **8**, 31 (1981)
5. Bryce, J. R., Venter, W. J. And Adam, J, In: D.O. Raush and B.C. Mariacher (Editors), *World Symposium on Mining and Metallurgy of Lead and Zinc*, Volume I, AIME, New York, N.Y., 542 (1970).
6. Gauci, G, A., In: D.O. Raush and B.C. Mariacher (Editors), *World Symposium on Mining and Metallurgy of Lead and Zinc*, Volume I, AIME, New York, N.Y., 373 (1970).
7. Ralston, J., Alabaster, P., and Healy, T.W., *International Journal of Mineral Processing*,**7**, 279, (1981)
8. Gardner , J.R., and Woods,R., .*International Journal of Mineral Processing*, **6**,1 (1979)
9. Finkelstein, N.P., *International Journal of Mineral Processing.*, **52**, 81 (1997).
10. Sutherland, K.L. and Wark, I.W., *Principles of Flotation*, Austr. IMM, 1955.
11. Wark, I.W. and Sutherland, K.L., *Am. Inst. Mining Met. Engrs.*, Tech. Pub. No. 1130, 23 (1939).
12. Steininger, J., *SME: Trans. AIME*, 241, 34 (1968).
13. Girczys, J.S. Laskowski and J. Lekki, *Can. Metallurgical Quarter*, **11**, 553 (1972).
14. Laskowski, J.S., Liu, Q. And Zhan, Y., *Minerals Engineering*, **10,** 787 (1997).
15. Israelachvili, J.N., and Adams, G.E., J.Chem.Soc. Faraday Trans.1., **74**, 975 (1978)
16. Israelachvili, J., and Pashley, R.M., *Nature*, 300, 341 (1982)
17. Horn, R.G., Smith, D.T., and Haller, W., Chem. Phys. Lett. 162, 404 (1989)
18. Pashley, R.M., Mcguiggan, P.M., Ninham, B.W., and Evans, D.F., *Science*, **229**, 1088
19. Claesson, P.M., Blom, C., Herder, C.E., and Ninham, B.W., *J.Colloid Interface Sci.* **239**, 234 (1986)
20. Christenson, H.K and Claesson, P.M., *Science*, **239**, 390 (1988)
21. Yoon, R.-H., and Ravishankar, S. A., *J.Colloid Interface Sci.* **179**, 391
22. Wood, J., and Sharma, R., *Langmuir*, **11**, 4797 (1995)
23. Tsao, Y-H., Evans, D.F., and Wennerstrom, H., *Science*, **262**, 547 (1993)
24. Ducker, W.A, Senden, T.J., and Pashley, R.M., *Nature*, **353**, 239 (1993)
25. Rabinovich, Ya. I., and Yoon, R-H, *Colloids and Surfaces*, **93**,263 (1994).
26. Yoon, R-H., Flinn, D.H., and Rabinovich, Ya.I., *J.Colloid Interface Sci.*, **185**, 179 (1997)
27. Toikka, G., and Hayes, R.A., *J.Colloid Interface Sci.*, **191**, 102 (1997)
28. Yoon, R-H., and Vivek, S., *J.Colloid Interface Sci.*, **204**, 179 (1998)
29. Ducker, W.A., Xu,Z., and Israelachvili, J.N., *Langmuir*, **10**, 3279 (1994)
30. Butt, H-J., *J.Colloid Interface Sci.* **166,** 109 (1994)

31. Fielden, M.L., Hayes, R.A., Ralston, J., *Langmuir*, **12**, 3721 (1996)
32. Preus, M., and Butt, H.J., *Langmuir*, **14**, 3164 (1998)
33. Flinn, D. H., *Ph.D. Dissertation*, Virginia Polytech. Institute & State Univ., (1996)
34. Yoon, R-H. and Pazhianur, R., *Colloids and Surfaces*, **144**, 59 (1998)
35. Blake and Kitchener., *J. Chem. Soc. Faraday Trans. 1*, **68,** 1435 (1972)
36. Craig, V.S., Ninham, B.W., and Pashley, R.M., *J.Phys. Chem*,**97**, 10192 *(1993)*
37. Aksoy, S., and Yoon, R-H., *J. Colloid and Interface Sci*., In press.
38. Parker, J.L., Claesson, P.M., and Attard, P., *J.Phys. Chem*., **98**, 8468 (1994).
39. Pugh, R.J. and Yoon, R-H, *J. Colloid Interface Sci.* **163,** 169 (1994).
40. Quan, D., Freysz, E., and Ron Shen, Y., *Science*, **264**, 826 (1994)
41. Nalaskowski, J., Veeramasuneni, S., and Miller, J.D, In: Atak, S., Onal, G., Celik, M.S., Balkema/Rotterdam/Brookfield, "Innovations in Mineral and Coal Processing", 159 (1998).
42. Derjaguin, B.V., and Landau, L., USSR Acta Physiochim. **14**, 633 (1941)
43. Verwey, E.J., and Overbeek, J.Th.G., "Theory of the Stability of Lyophobic Colloids, Elsevier, New York, 1947
44. Derjaguin, B.V. and Churaev, N.V., *Colloids and Surfaces*, **41**, 223 (1989).
45. Claesson, P.M., and Christenson, H.K., *J.Phys.Chem*., **92**, 1650 (1988).
46. Atkins, D. T., and Pashley, R. M., *Langmuir*, **9**, 2232 (1993).
47. Muster, T.H., Toikka, G., Hayes, R.A., Prestidge, C.A., Ralston,J, *Colloids and Surfaces*, **106,** 203 (1996).
48. Toikka, G., Hayes, R.A. and Ralston, J., *Langmuir*, **12**, 3783 (1996).
49. Toikka, G., Hayes, R.A. and Ralston, J., *Colloids and Surfaces*, **141**, 3 (1998).
50. Drelich, J., Laskowski, J.S., Pawlik, M., and Veeramasuneni, S., *J. Adhesion Sci.Technol*., **11**, 1399 (1997).
51. Flinn, D. H., Guzonas,D. A., and Yoon, R.-H., *Colloids and Surfaces*, **87**, 163 (1994).
52. Senden, T. J and Ducker, W. A, *Langmuir*,**10**, 1003 (1994)
53. Xu, Z., and Yoon, R.-H., *J. Colloid Interface Sci.* **132,** 532 ((1989).
54. Fowkes, F. M., *Ind. Eng. Chem*. **56**, 40 (1964).
55. Yoon, R-H., Chen, Z., Finkelstein, N.P., and Richardson, P.R., *XIX IMPC, SME*, 1995
56. The algorithm originally written by Alexis Grabbe was kindly lent to us by William Ducker.
57. Larson, I., Drummond, C.J., Chan, D.Y.C., and Grieser, F., *J.Phys.Chem*., **99**, 2114 (1995).
58. Meagher, L and Pashley, R., *J. Colloid Interface Sci.* **185,** 291 (1997).
59. Larson, I., Drummond, C.J., Chan, D.Y.C., and Grieser, F., *Langmuir*., **13**, 2109 (1997).
60. Toikka, G., and Hayes, R.A, *J. Colloid Interface Sci.* **191,** 102 (1997).
61. Laskowski, J.S and Kitchener, J.A., *J. Colloid Interface Sci.* **29,** 670 (1969).
62. Hough, D.B., and White, L.R., *Adv. Colloid and Interface Science*, **14**, 1980, 3
63. Parker, J.L., and Claesson, P.M., Langmuir, **10**, 635 (1994).
64. Meagher, L and Pashley, R., *Langmuir*., **11,** 4019 (1995).
65. Tsao, Y-H., Evans, F.D., and Wennerstrom, H., *Langmuir*, **9**, 779 (1993).
66. Chen, Z., and Yoon, R-H., *Submitted to International Journal of Minerals Processing*, 1997
67. Young, C., Masters Thesis, Virginia Polytechnic Institute and State University, 1987
68. Coleman, R.E., Powell, H.E., and Cochran, A.A., *Trans. SME*, 408, (1967)
69. Popov, S.R., and Vucinic, D.R., *Colloids and Surfaces*, **47**, 81 (1990).

70. Prestidge, C.A., Thiel, A.G., Ralston, J., Smart, R.St.C., *Colloids and Surfaces*, **85**, 51 (1994).
71. Yoon, R-H., and Mao, L., *J. Colloid Interface Sci*., **181,** 613 (1996).
72. Lekki, J., and Laskowski, J., *Trans.IMM* **80**, 174 (1971).
73. Groppo, J.G., Jr., and Yoon, R-H., Proceedings, the Engineering Foundation Conferemnce, Interfacial Phenomena in Mineral Processing, Rindge, New Hampshire, August 2-7, 1981,; Eds: B. Yarar and D. Spottiswood, 271 (1982).
74. Yucesoy, A and Yarar, B., *Trans. IMM.*, **84**, C 96 (1974).
75. Chen, Z., *Ph.D. Dissertation*, Virginia Polytechnic Institute and State University, 1998
76. Iwasaki, I., and Cooke, S.R.B., "The Decomposition of Xanthate in Acid Solution", *J.Am.Chem.Soc.* 80, (1958) 285
77. Tipman,, R.N., and Leja, J, *Colloid and Polymer Science*, **253**, 4 (1975)
78. Craynon, J., *Masters Thesis*, Virginia Polytechnic Institute and State University, 1985
79. Finkelstein, N.P., Allison, S.A., Lovell, V.M., and Stewart, B.V., *Advances in Interfacial Phenomena of Particulate/Solution/Gas Systems; Application to Flotation Research*, Eds: Somasundaran, P., and Grieves, R.B., A.I.Ch.E.: New York, Chem. Eng. Prog. Symposium Series No.13, (1975).
80. Yoon, R-H., and Chen, Z., *In: Proc.Int.Symp.Electrochemistry in Mineral and Metal Processing IV*,Richardson, P.E., Srinivasan,S., and Woods, R.Eds., Electrochem.Soc.Pennington,N.J.,38 (1996).
81. Laskowski,J., *Advances in Mineral Processing, Ed: Somasundaran, P., SME Inc.*, 189 (1986).

Table 3.1. Results of the Direct Surface Force Measurements Conducted with Activated Sphalerite and Unactivated Sphalerite under Different Conditions

pH	Reagent Additions	Contact Angle (θ)	K_{132} (10^{-19} J)	K_{131} (10^{-20} J)*
9.2	KEX	16	-	-
	$CuSO_4$+KEX	65	30.0	4.5
6.8	KEX	15	-	-
	$CuSO_4$+KEX	20	-	-
4.6	KEX	15		
	$CuSO_4$+H_2O_2	41	7.0	0.25
	$CuSO_4$+H_2O_2+KEX	49	12.0	0.72

* obtained from K_{132} using Eq.[8] with $K_{232}=2\times10^{-16}$ J

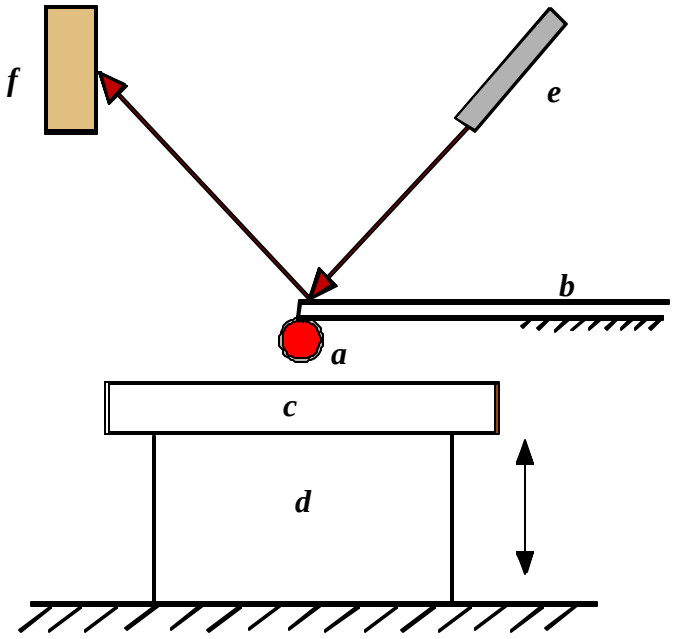

Figure 3.1. A schematic representation of the working principle of the atomic force microscope (AFM) used for surface force measurements: a) hydrophobized glass sphere; b) cantilever; c) mineral plate; d) piezo-electric crystal; e) laser source; f) photo diode. The measurement is conducted in aqueous solutions.

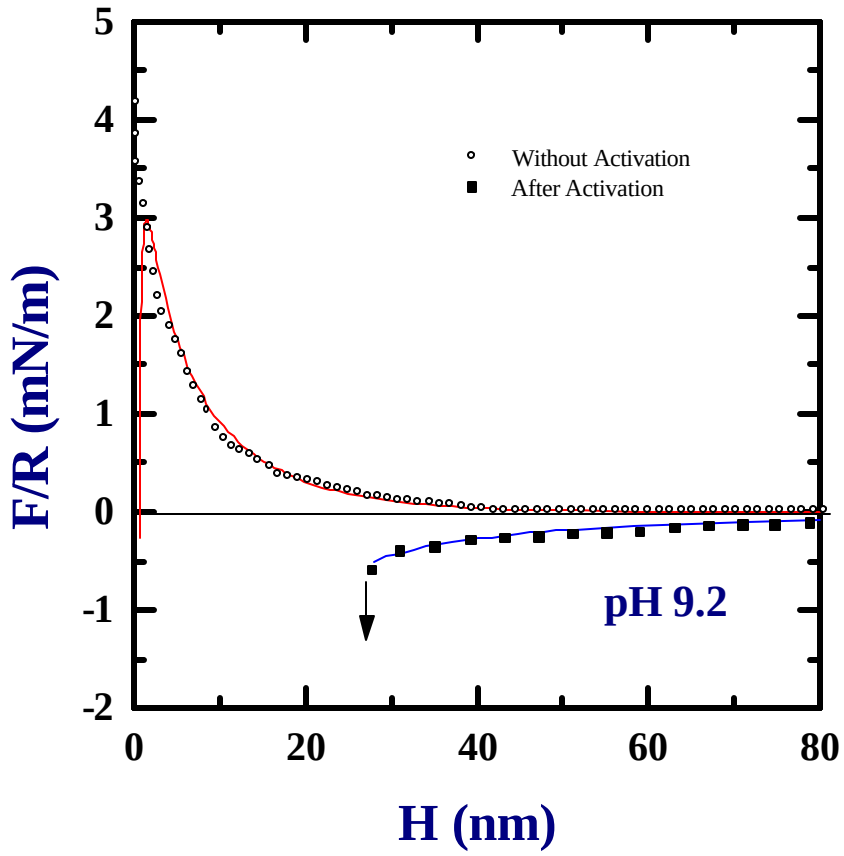

Figure 3.2. The *F/R* vs *H* curves obtained for the interaction between a polished sphalerite plate and a hydrophobic glass sphere (q=109°) in 10^{-3} M KEX solutions at pH 9.2. The upper force curve shows the results obtained with unactivated sphalerite. The upper solid line represents the DLVO fit (constant charge model) to the data with $y_{1(\infty)}$(sphalerite) = −63 mV; $y_{2(\infty)}$(glass sphere) = −60 mV, κ^{-1}= 9.1 nm, and A_{132}=0.8×10^{-20} J. The good fit indicates that the unactivated sphalerite does not exhibit hydrophobic forces. The lower force curve shows the results obtained with copper-activated sphalerite. The data can be fitted to the extended DLVO theory (Eq. [3]) which incorporates a hydrophobic force term (Eq. [4]) with K_{132}=3.0×10^{-18} J. Other force parameters are the same as those used for the unactivated sphalerite.

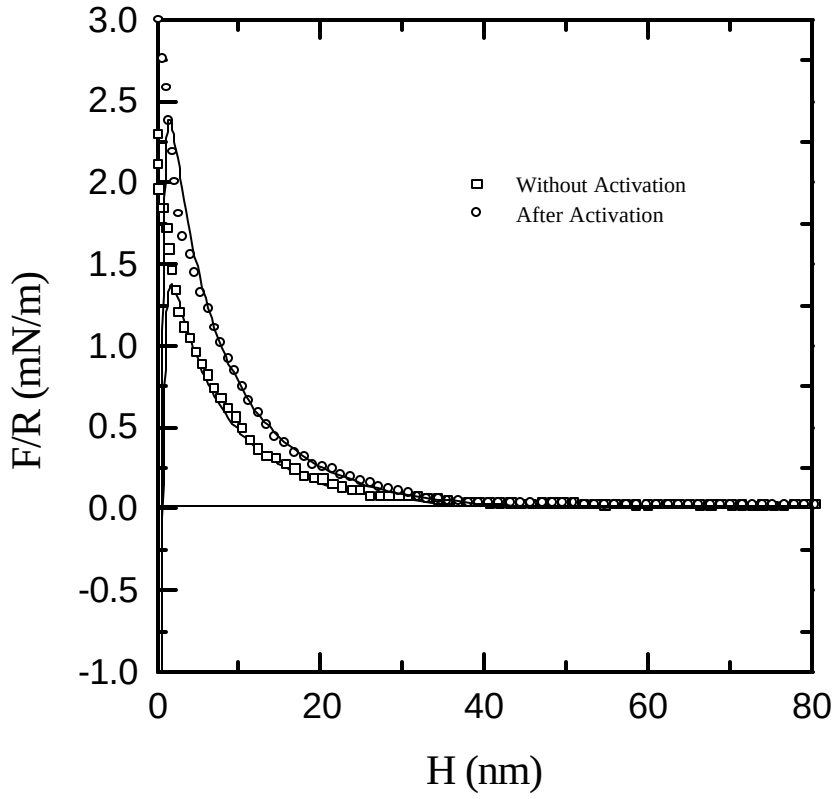

Figure 3.3. The *F/R vs H* curves obtained for the interaction between polished sphalerite plate and hydrophobic glass sphere (θ=109°) in 10^{-3} M KEX at pH 6.8. The lower curve represents the data obtained with unactivated sphalerite, which have been fitted to the DLVO theory (constant charge model) with $\psi_{1(\infty)}$=−34 mV, $\psi_{2(\infty)}$=−54 mV, κ^{-1}=9.8 nm, and $A_{132}=0.8\times10^{-20}$ J. The upper curve represents the data obtained with copper-activated sphalerite with $\psi_{1(\infty)}$=−51 mV, $\psi_{2(\infty)}$=−54 mV, κ^{-1}=10.1 nm, and $A_{132}=0.8\times10^{-20}$ J. The higher negative surface potential of the activated sphalerite probably indicates the adsorption of xanthate.

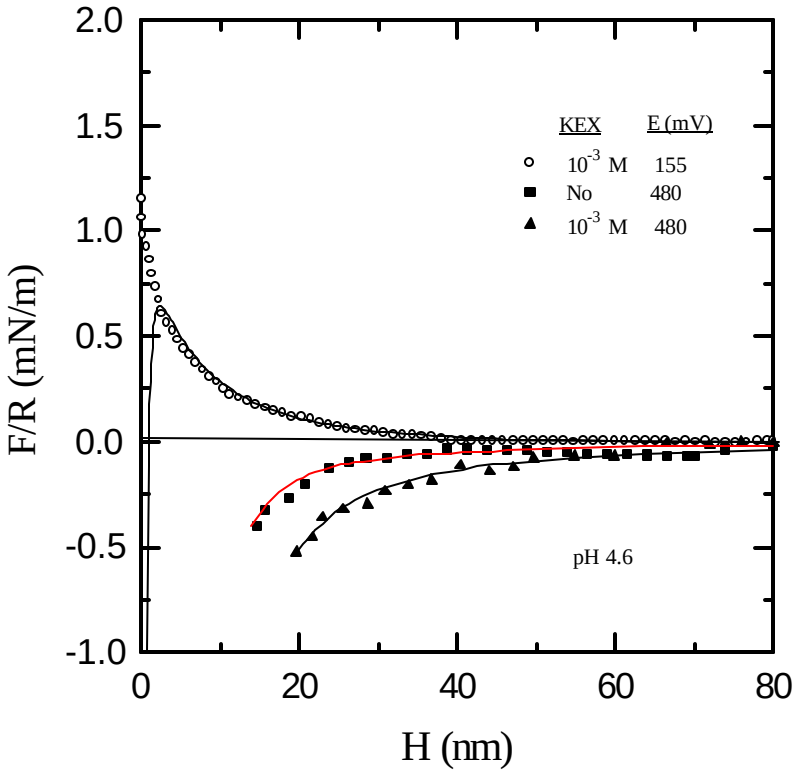

Figure 3.4. The *F/R vs H* curves obtained for the interaction between copper-activated sphalerite plate and hydrophobic glass sphere (q=109^0) at pH 4.6. The force data (▲) obtained in a 10^{-3} M KEX solution at 155 mV can be fitted to the DLVO theory (upper solid line) with $y_{1(\infty)}$=−25 mV, $y_{2(\infty)}$=−40 mV, κ^{-1}=12.4 nm, A_{132}=0.8×10^{-20} J. When the potential was raised to 480 mV (●), net attractive forces were observed. The data have been fitted to the extended DLVO theory (Eq. [3]) which incorporates a hydrophobic force term (Eq. [4]) with K_{132}=1.2×10^{-18} J. Other fitting parameters are the same as those used for the data obtained at 155 mV. The data obtained at 480 mV in the absence of KEX (■) have been fitted to the extended DLVO theory with K_{132}=7×10^{-19} J.